

Characterization of poly(1-butene) surfaces by scanning tunneling microscopy

H. Fuchs¹, L. M. Eng¹, R. Sander¹, J. Petermann^{2*}, K. D. Jandt², and T. Hoffmann²

¹BASF AG, Polymer Research Division, ZKL/T – J 543, W-6700 Ludwigshafen,
Federal Republic of Germany

²TU Hamburg-Harburg, Polymer Composites Group, Harburger Schloßstrasse 20,
W-2100 Hamburg 90, Federal Republic of Germany

Abstract

Poly(1-butene) (PB-1) films drawn from the melt have been deposited on highly oriented pyrolytic graphite (HOPG) substrates for investigation with the scanning tunneling microscope (STM). The STM investigations showed images of PB-1 flakes extending over some hundred nanometers. Their thickness was determined to be much larger than the normal tunneling distance established between the tip and a good conducting (metallic) sample surface. Close to monomolecular film steps, our STM measurements simultaneously revealed both the atomic resolution of the HOPG substrate and a superlattice showing an ordered structure pseudomorphic to the helical nature of the PB-1 macromolecule.

Introduction

The crystal structure of isotactic poly(1-butene) and many other polymer crystals is well known (1,2). However, the knowledge about the surface of polymeric crystals is less elaborated. What may be observed on such surfaces are effects like relaxations or reconstructions which are not well explored. The surface of uniaxially oriented semicrystalline polymeric thin films is of particular interest especially for an understanding of interfacial and surface effects (3). To answer (some of) these questions, the use of a STM (4) is well recommended because of its surface sensitivity i.e. its capability to directly image the local electronic surface states. This makes it an excellent complementary method for TEM investigations (3) probing the bulk properties. For good imaging of organic films (5,6,7), an essential premise is either a sufficiently high electrical conductivity (8) or films of such a small thickness that the molecules fit spacially into the tunneling gap (9) thereby modulating either the electronic density of states of the substrate material or the tunneling barrier height.

*To whom offprint requests should be sent

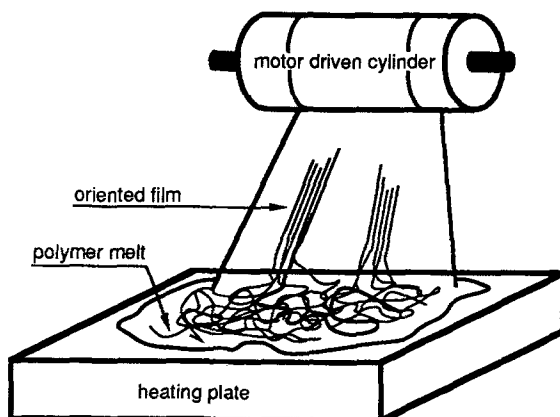


Fig. 1: Schematic diagram demonstrating the preparation method of oriented PB-1 thin films

Experimental

The oriented semicrystalline PB-1 substrates are prepared according to the method of Petermann and Gohil (10): PB-1 is dissolved in xylene (~ 0.4 %). Some droplets of this solution are then deposited on the smooth surface of a glass slide where the solution itself disperses uniformly. When heating the sample to a temperature of about 130-140°C, the solvent evaporates. From the resulting melt (thickness $\leq 1 \mu\text{m}$) a highly oriented ultra thin film is drawn (with a thickness below 20 nm) by a motor driven cylinder ($v_x \approx 7 \text{ cm/sec}$) (Fig.1). In case of careful preparation, even thinner films can be produced by this technique. The samples were then prepared in two different ways: for transmission electron microscopic (TEM) investigations, the oriented film is cut into pieces and mounted onto copper grids, while for the STM investigations, the PB-1 films were fixed on a HOPG substrate.

Results and Discussion

Electron microscopic investigations with a Philips 400 T operated at 100 kV showed that the PB-1 film consists of crystalline and amorphous regions. The crystalline areas are made up from needle like crystals with dimensions ranging from a few nm to some μm in length and a diameter of about 10 nm. Within the amorphous regions, no strict crystallographic order is seen. Nevertheless, it is possible that some parts of the macromolecules are unidirectionally oriented. The orientation of the crystallites and macromolecules in the films is caused by the extension of the melt. Fig. 2 presents a platinum shaded surface of a PB-1 thin film. It shows elongated elevations measuring some ten nanometers in length and a few nm in height, respectively. It is proposed that these structures originate from the needle like crystals protruding

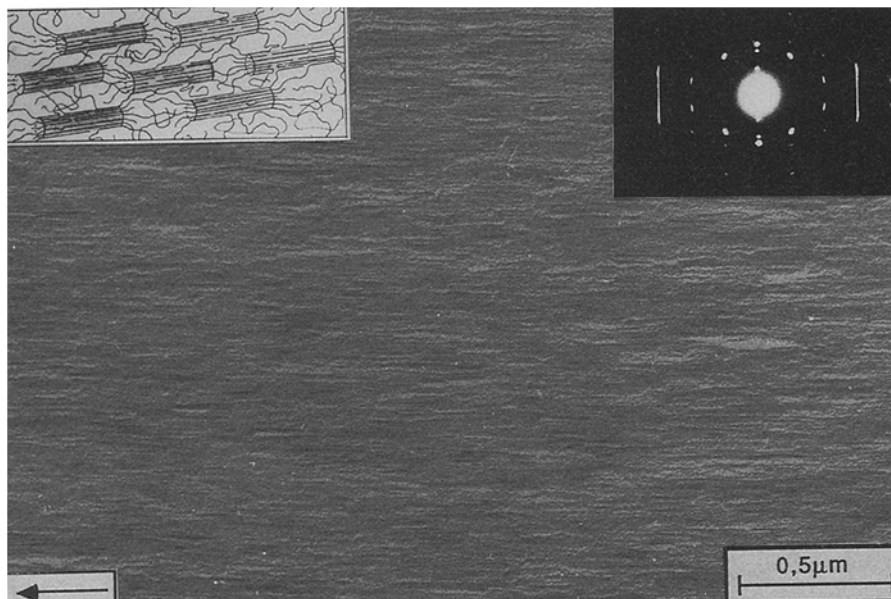


Fig. 2 : TEM picture of a Platinum shaded PB-1 film surface. The arrow in the lower left corner demonstrates the direction of the molecular orientation. An electron diffraction pattern and a sketch of the morphology are inserted

out of the sample surface. From electron diffraction patterns of the PB-1 film (inset in Fig. 2), we deduce that the crystalline conformation of the macromolecules build up a $2 \times 3_1$ helix with an identity period of about 6.5 Å. PB-1 crystals exhibit a rhombohedral unit cell with an identity period of each hexagonal axis of 17.7 Å (stable structure) (1). As described above, the PB-1 thin films are not of single crystalline order but rather show a fibrillar arrangement of individual crystals which have in common one crystallographic axis only, the direction of the molecular orientation (fibre texture). For such crystals the lowest distance of two chains in an (hk0)-plane is about 6 Å. The ratio calculated from the identity period of the PB-1 chain and the smallest distance between two chains is about 1.1.

Fig. 3 depicts a view of the tunneling microscope to a $250 \times 250 \text{ nm}^2$ surface spot revealing the PB-1 polymer film deposited onto HOPG. This image shows some extended PB-1 flakes; at the position marked with an arrow the tunneling tip has touched the sample thereby probably turning over some of the PB-1 flakes. The flakes themselves depict the fibrillar structure of the PB-1 film as best seen from edge regions of flakes at the film/substrate interface. Surprisingly, it was easily possible to image these flakes with STM although their thickness of about 80 Å rather implies the insulating



Fig. 3: STM image of a PB-1 film deposited onto HOPG. Imaging was done in air over an area of $250 \times 250 \text{ nm}^2$, $I_t = 0.6 \text{ nA}$, $V_t = 463 \text{ mV}$, tip positive. The extended flakes consist of polymeric material. Note the fibrillar structure of the film at the edge of the flake.

character as found in the bulk material (11). The good conductivity thus can only be understood when the top layer of the film is thought to be sufficiently conductive (probably due to contamination with H_2O or carbon from the HOPG substrate), or when the high electric field strength locally

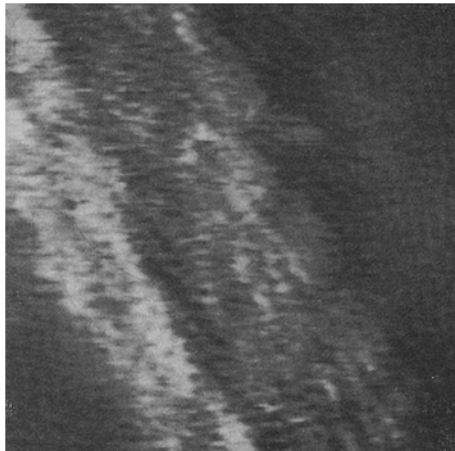


Fig. 4: STM image with increased magnification compared to Fig. 3, magnifying the fibrillar structure of the PB-1 film. Image size is $8.8 \times 9.8 \text{ nm}^2$, $I_t = 0.6 \text{ nA}$, $V_t = 463 \text{ mV}$

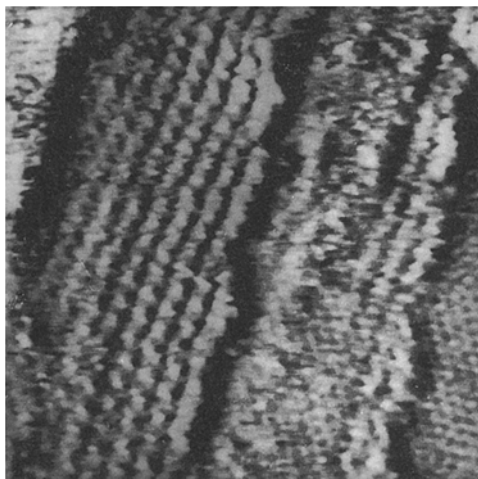


Fig. 5: High resolution STM picture of a HOPG surface patch covered with the PB-1 film. In the lower right corner the atomically resolved lattice of graphite is visible. The helical structure originating from the PB-1 film filaments has a pitch height of $\sim 3.8 \text{ \AA}$. The distance between two helices is measured to be 4.2 \AA . $I_t = 1 \text{ nA}$, $V_t = 160 \text{ mV}$, image size: $7.5 \times 9.2 \text{ nm}^2$

induces an enhanced mobility of charge carriers along molecular fibrilles of the material. Nevertheless, the surface shown in Fig.3 provided stable conditions while imaging with STM.

When imaging on thinner parts of the PB-1 film (i.e. closer at the film/substrate interface) at a higher magnification, our STM recorded the fibrillar structure presented in Fig.4. When imaging at an even higher magnification on surface spots covered essentially with monolayers of parallel aligned molecular helices, pictures as presented in Fig.5 were obtained. In the lower right corner of this image, the atomic structure of the bare graphite substrate is imaged. The measured interatomic spacing of 2.46 \AA can well be used as a direct calibration standard when investigating the helical structure originating from the PB-1 films. When calculating the ratio measured from the pitch height of helices and the medium distance between two helices, a ratio of 0.9 is obtained, in fairly good agreement with the bulk value (1). However, the measured interhelical distance of $\sim 4.2 \text{ \AA}$ is much smaller (about 1/3) than the expected value of about 6 \AA . Therefore, if the observed structure is real, the presence of the substrate lattice must have taken dramatic influence on the packing or the molecular array.

Another explanation would treat the measured superstructure as a pure electronic effect with the molecular helices originating from the interference between the graphite substrate lattice and the PB-1 film (12). This hypotheses

would be supported by the fact that helical structures recorded in a series of pictures similar to Fig.4 and Fig.5 gradually decay into the graphite lattice parallel to the surface rather than ending abruptly, for example, at the rightmost helix of a molecular bundle. Thus, at present, an electronic effect yielding the 'atomic' resolution of molecules cannot be ruled out. A more detailed analysis investigating interfacial structural and electronic effects between molecular overlayers and conducting substrates is in progress and will be published elsewhere.

These first STM experiments on melt-drawn PB-1 polymer films rather aimed to investigate the feasibility of structural and electronic surface inspection with the STM as a complementary method to TEM. It was shown that fairly thick parts of the PB-1 films can be imaged, which similar to other organic materials, rise the question of local electrical conductivity in thin layers of bulk insulators. Furthermore, pictures have been obtained showing a helical (super-) structure as well as fine structures corresponding to the intra-molecular atomic distance of the helical structure of the PB-1 films.

Acknowledgement

H.F. and L.E. gratefully acknowledge support by a materials research project by the BMFT under grant number 03M4008BO and J.P. and K.D.J. gratefully acknowledge the financial support of the Volkswagen Foundation.

References

1. Natta G, Corradini P, and Bassi I W (1960) Suppl. Nuovo Cimento 15 (10): 52
2. Wunderlich B (1973) Macromolecular Physics, Vol. 1, Academic Press, New York
3. Petermann J, Broza G (1987) J. Mater. Sci. 22: 1108
4. Binnig G, Rohrer H (1982) Helv. Phys. Acta 55: 726
5. Fuchs H., Akari S and Dransfeld K (1990) Z. Phys. B - Condensed Matter 80: 389
6. Michel B, Travaglini G, Rohrer H, Joachim C and Amrein M (1989) Z. Phys. B - Condensed Matter 76: 99
7. Reneker D H, Schneir J, Howell B and Harary H (1990) Polymer Communications 31 (5): 167
8. See for example:
Fuchs H, Schrepp W (1989) Surface Characterization of Thin Organic Films by Scanning Tunneling Microscopy. In: Saegusa T, Higashimura T, Abe A (ed.) Frontiers of Macromolecular Science. Blackwell Scientific Publications (Proc. MACRO '88, Kyoto, pp 499)
9. Ohtani H, Wilson R J, Chiang S and Mate C M (1988) Phys. Rev. Lett. 60: 2398
10. Petermann J, Gohil R M (1979) J. Mater. Sci. 14: 2260
11. Dietz P, Hermann K-H (1990) Surf. Sci. 232: 339
12. Mizes H S, Foster J S (1989) Science 244: 559